

Latent Neural Ordinary Differential Equations for Model-Informed Precision Dosing: Overcoming Structural Assumptions in Pharmacokinetics

Benjamin Maurel^{*1}, Agathe Guilloux¹, Sarah Zohar¹, Moreno Ursino¹, and Jean-Baptiste Woillard^{5,6}

¹Université Paris Cité, Inria, Inserm, HeKA, F-75015 Paris, France

⁵Université de Limoges, CHU Limoges, P&T, U1248, Limoges, France

⁶Service de Pharmacologie, Toxicologie et Pharmacovigilance, CHU Limoges, France

Abstract

Accurate estimation of tacrolimus exposure, quantified by the area under the concentration–time curve (AUC), is essential for precision dosing after renal transplantation. Current practice relies on population pharmacokinetic (PopPK) models based on nonlinear mixed-effects (NLME) methods. However, these models depend on rigid, pre-specified assumptions and may struggle to capture complex, patient-specific dynamics, leading to model misspecification. In this study, we introduce a novel data-driven alternative based on Latent Ordinary Differential Equations (Latent ODEs) for tacrolimus AUC prediction. This deep learning approach learns individualized pharmacokinetic dynamics directly from sparse clinical data, enabling greater flexibility in modeling complex biological behavior. The model was evaluated through extensive simulations across multiple scenarios and benchmarked against two standard approaches: NLME-based estimation and the iterative two-stage Bayesian (it2B) method. We further performed a rigorous clinical validation using a development dataset ($n = 178$) and a completely independent external dataset ($n = 75$). In simulation, the Latent ODE model demonstrated superior robustness, maintaining high accuracy even when underlying biological mechanisms deviated from standard assumptions. Regarding experiments on clinical datasets, in internal validation, it achieved significantly higher precision with a mean RMSPE of 7.99% compared with 9.24% for it2B ($p < 0.001$). On the external cohort, it achieved an RMSPE of 10.82%, comparable to the two standard estimators (11.48% and 11.54%). These results establish the Latent ODE as a powerful and reliable tool for AUC prediction. Its flexible architecture provides a promising foundation for next-generation, multi-modal models in personalized medicine.

Code availability: The source code and pre-trained models are available at <https://github.com/BenJMaurel/PharmaNODE>.

Keywords: Pharmacokinetics, Neural ODE, Deep Learning, Tacrolimus, Precision Medicine

1 Introduction

Model-Informed Precision Dosing (MIPD) aims to improve drug therapy by adapting treatment to individual patients rather than relying on prespecified fixed dosing strategies for all patients. By leveraging mathematical models, MIPD seeks to capture patient-specific drug behavior over time, enabling more accurate and safer dosing decisions during patient’s follow-up. This challenge finds an important application in renal transplantation, a life-saving treatment for end-stage renal

^{*}Corresponding author: benjamin.maurel@inserm.fr

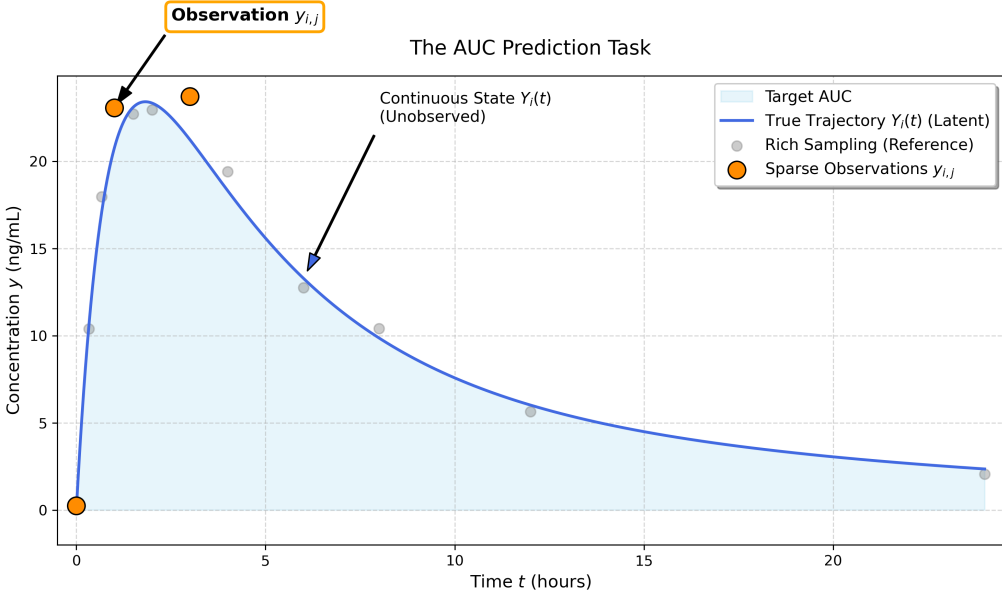


Figure 1: **The AUC Prediction.** The blue curve represents the patient’s true underlying drug concentration over time, and the shaded area corresponds to the target AUC we wish to estimate. The grey dots illustrate a rich sampling strategy (e.g., 12 samples - each point with a measurement error), which allows for accurate AUC estimation but is impractical in routine clinical care. In contrast, only a few measurements (orange points, collected at 0 h, 1 h, and 3 h) are typically available. The objective is to estimate the full 24h-AUC from these limited observations.

disease. Long-term graft survival depends heavily on lifelong immunosuppressive therapy, most commonly with tacrolimus. Despite its effectiveness, tacrolimus is a notoriously difficult drug to manage because its therapeutic window, that is, the difference between an effective and a harmful exposure, is small. Insufficient exposure may lead to immune rejection and graft loss, whereas excessive exposure can cause serious adverse effects, including nephrotoxicity and neurotoxicity. To stay within this safe window, clinicians must monitor the patient’s exposure. The most reliable metric in this clinical setting to quantify this exposure is the Area Under the Curve (AUC; see Figure 1) of the concentration-time trajectory [1, 2]. Ideally, achieving a good approximation of the AUC from noisy drug concentrations requires ‘rich sampling’ drawing blood 8 to 12 times over a 24-hour period (see Figure 1). In routine clinical practice, this is invasive, costly, and logically impractical. Instead, clinicians rely on a limited sampling strategy, collecting only a few blood samples (e.g., 2 or 3 points) and using mathematical models to reconstruct the full exposure curve [3, 4].

Historically, the reconstruction of drug exposure from limited clinical measurements has relied on nonlinear mixed-effects (NLME) models, also referred to as population pharmacokinetic (PopPK) models [5, 6, 7, 8]. These parametric models describe drug dynamics using predefined mechanistic equations shared across patients, with inter-individual variability captured through random effects in some model parameters. While effective in many clinical settings, their performance depends on the validity of the assumed structural form and on the ability to estimate the model parameters. When pharmacokinetic behavior deviates from these assumptions, due, for example, to complex metabolic processes, unobserved biological factors, or drug–drug interactions, model flexibility may be limited, and transferability to external populations can be reduced [9].

In this work, we introduce a deep learning framework based on Latent Ordinary Differential Equations (Latent ODEs) [10, 11]. This approach models patient trajectories in continuous

time, allowing it to naturally accommodate sparse observations and irregular sampling, a common burden with clinical data. More importantly, the fact that the dynamic of these differential equations is driven by a neural network allows for a more flexible, nonparametric estimation strategy. Although we focus on tacrolimus as a clinically relevant use case, the proposed framework is broadly applicable to pharmacokinetic modeling problems involving limited and irregular measurements.

Contributions We propose a novel data-driven framework for pharmacokinetic modeling that addresses several key limitations of existing approaches. In particular, in this work:

1. **Methodological Innovation:** We introduce a Latent ODE framework with a Gaussian Mixture prior designed specifically for pharmacokinetics. Unlike standard Neural ODEs, this architecture separates patient-specific variability (latent state) from the governing dynamics, allowing for a learnable, structured representation of patient heterogeneity.
2. **Robustness to Misspecification:** Through a comprehensive simulation study, we demonstrate that our data-driven approach maintains high predictive accuracy even when the underlying biological mechanism deviates from standard assumptions (e.g., saturation kinetics or missing covariates), a scenario where traditional parametric models exhibit significant bias.
3. **Rigorous Clinical Validation:** We validate the model on two real-world datasets, including a completely unseen external cohort. We show that the Latent ODE achieves precision comparable to gold-standard estimators without requiring any pre-specified structural equations.
4. **Interpretability and Open Science:** We show that the learned latent space organizes patients into physiologically meaningful clusters (e.g., by genotype and formulation) in a completely unsupervised manner. Finally, we make our full training pipeline and pre-trained models publicly available to foster reproducibility.

2 Related Work

The clinical standard for MIPD and AUC estimation relies on parametric PopPK modeling. However, the performance of these frameworks heavily depends on the validity of the structural assumptions [9]. In this section, we review the conceptual foundations of these standard approaches before introducing the data-driven Neural ODE framework.

2.1 Parametric Paradigm: Nonlinear Mixed-Effects Models

The standard framework for describing population pharmacokinetics is the NLME model [12, 13]. This modeling framework is parametric: it assumes that the observed data are generated by a fixed, pre-specified mechanistic structure, typically a system of compartmental differential equations chosen by domain experts (detailed in Supplementary Materials). In this framework, patient variability is handled hierarchically. The model assumes a typical patient profile defined by fixed population parameters (e.g., mean clearance), while individual deviations from this value are captured by random effects. While this approach is powerful when the biological mechanism is well-understood, it is rigid by design: the model can only fit data patterns allowed by the pre-chosen mathematical structure.

Once the structural model is fixed, specific algorithms are required to estimate the parameters. Even though fully Bayesian inference has become increasingly appealing in recent years for estimating NLME models [14], the most widely used inference framework remains the frequentist one, at least for the fixed-effects component. Therefore, the most common academic approach

involves a two-step procedure in which fixed effects are first estimated via marginal likelihood, and individual random effects are subsequently retrieved. Population parameters are estimated by maximizing the likelihood of the observed data, commonly using linearization-based methods such as First-Order Conditional Estimation (FOCE) [15] or Stochastic Approximation Expectation Maximization, including the SAEM algorithm [16]. In general, the individual parameters for a specific patient are then estimated using a Bayesian method, namely the Empirical Bayes Estimation (EBE) approach, computed under the assumption that all PPK model parameters are known without uncertainty [17, 18]. In particular, in this work we use the Maximum A Posteriori Bayesian Estimator (MAP-BE) [3] as the EBE following estimation via the SAEM algorithm. This estimator searches for the most probable parameters for a new patient by balancing the fit to their sparse data against the population prior. Crucially, this optimization is strictly constrained by the pre-specified structural equations; if the model structure is misspecified, the estimator will force the data to fit an incorrect curve.

The Iterative Two-Stage Bayesian (IT2B) method [19] is an alternative strategy widely used in clinical software (e.g., the ISBA benchmark used in this study). Unlike the sequential SAEM approach, IT2B estimates individual and population parameters iteratively. While computationally distinct, it remains a parametric method subject to the same structural limitations as before.

2.2 Deep Learning and Neural ODEs

To overcome the constraints of rigid structural assumptions, machine learning (ML) approaches were proposed in literature. Early efforts utilized static models, such as Xgboost or standard Neural Networks, to map patient covariates directly to clinical endpoints [20]. However, these “static” models ignore the continuous temporal nature of drug concentration and cannot easily handle irregular sampling times.

A significant breakthrough in modeling dynamics was the introduction of Neural Ordinary Differential Equations (Neural ODEs) [10]. Instead of requiring an expert to write down the differential equations governing the system (as in NLME), Neural ODEs use a neural network to learn the derivative function (i.e the dynamic) directly from data and naturally handles irregular sampling times.

Recent works have demonstrated the utility of this approach in pharmacokinetics. Lu et al. (2021) [21] presented one of the first application of Neural ODEs to pharmacokinetics, demonstrating that they outperform standard recurrent networks in generalizing predictions to untested dosing regimens (e.g., training on a once-every-three-weeks schedule and predicting outcomes under a once-weekly schedule) using as input an entire PK cycle data and trying to predict the subsequent ones. Addressing data scarcity, Bräm et al. (2023) [22] proposed “low-dimensional” Neural ODEs. To prevent overfitting, they explicitly restrict the neural network to operate on a very small number of state variables. While effective for regularization, this method remains a deterministic model. More recently, Giacometti et al. (2025) [23] leveraged Neural ODEs to handle complex covariate relationships and improve explainability via SHAP (SHapley Additive exPlanations) values [24], relying on data augmentation to stabilize training.

Our work differs fundamentally from these contributions by adopting a generative probabilistic framework via a Variational Auto-Encoder (VAE) Latent-ODE based architecture [11]. This architecture embeds the Neural ODE within a probabilistic generative model, allowing it to handle the noise, sparsity, and irregularity inherent in medical time-series. By learning the dynamics rather than imposing them, this approach offers a nonparametric alternative for AUC prediction that can adapt to complex, non-standard biological behaviors.

3 Model

We consider a dataset of N independent subjects. We assume that the drug pharmacokinetics for subject i follow an underlying, unobserved continuous process $Y_i(t)$. We assume that the observations $y_{i,j}$ are noisy realizations of the underlying true continuous trajectory $Y_i(t)$:

$$y_{i,j} = Y_i(t_{i,j}) + \epsilon_{i,j}, \quad \text{with } \epsilon_{i,j} \sim \mathcal{N}(0, \sigma_{obs}^2). \quad (1)$$

In our experimental setting (both simulation and clinical validation), we have access to a rich sampling profile for each patient, denoted as $\mathcal{R}_i = \{(t_{i,k}, y_{i,k})\}_{j=1}^{M_i}$, where M_i is the total number of available measurements (typically $M_i \approx 10 - 12$). These rich samples serve as the ground truth reference for the concentration trajectory. However, the objective of this work is to predict exposure from limited data. Therefore, the model input consists only of a sparse subsample of observations, denoted as $\mathcal{O}_i \subset \mathcal{R}_i$. Formally, $\mathcal{O}_i = \{(t_{i,j}, y_{i,j})\}_{j=1}^{m_i}$, where $m_i < M_i$ (typically $m_i \approx 3$). Let s_i be a vector of subject-specific static covariates (e.g., genotype, age, administered dose d_i). The dataset used for modeling is thus $\mathcal{D} = \{(\mathcal{O}_i, \mathcal{R}_i, s_i)\}_{i=1}^N$. The model observes (\mathcal{O}_i, s_i) to estimate the trajectory, while \mathcal{R}_i is used solely to compute the loss during training or to validate the AUC predictions.

The clinical quantity of interest is the AUC, defined as the integral of the patient's true unobserved drug concentration trajectory $Y_i(t)$ over the dosing interval $(0, t^*)$,

$$\text{AUC}_i = \int_0^{t^*} Y_i(t) dt. \quad (2)$$

Depending on the formulation of tacrolimus used, $t^* = 12h$ or $24h$ (for more information on the two different formulation, see in Supplementary Materials). To simplify the next sections we will suppose $t^* = 12h$ from now on without any loss of generality. Our goal is to learn a model that reconstructs the continuous function $Y_i(t)$ from the sparse subset of longitudinal data \mathcal{O}_i and static baseline covariates s_i in order to compute the integral in Eq. 2.

3.1 The Generative Model

To overcome the rigid structural constraints of NLME, we propose a probabilistic generative model based on Latent Ordinary Differential Equations (Latent ODEs) [11]. Instead of modeling the drug concentration directly with fixed equations, we represent the patient's internal physiological state as an abstract latent variable $z_i(t)$.

The Prior (Initial State)

We assume the patient's entire physiological context at $t = 0$ is fully characterized by a latent initial state $z_0^i \in \mathbb{R}$. Since z_0^i cannot be observed directly, we define a prior distribution $p(z_0^i)$ defining the distribution for the population before seeing a specific patient's data. In standard settings, this prior is assumed to be Gaussian. To capture heterogeneity across subpopulations (e.g., genetic differences), we instead model the prior as a Gaussian Mixture Model (GMM),

$$p(z_0^i) = \sum_{k=1}^K \pi_k \mathcal{N}(z_0^i | \mu_k, \Sigma_k), \quad (3)$$

where π_k, μ_k, Σ_k are learnable parameters and K is a fixed hyper-parameter.

The Latent Dynamics

Given the initial state z_0^i , the evolution of the patient's latent state $z^i(t)$ is deterministic and governed by an Ordinary Differential Equation (ODE) parameterized by a neural network f_ϕ :

$$\frac{dz^i(t)}{dt} = f_\phi(z^i(t), t). \quad (4)$$

Unlike classical pharmacokinetics where f is fixed by experts, here f_ϕ is a learnable non-linear function. The state at any future time t is obtained by solving the initial value problem:

$$z^i(t) = z_0^i + \int_0^t f_\phi(z^i(\tau), \tau) d\tau. \quad (5)$$

Eq.5 can be easily solved via any integration routine.

The Observation Model (Likelihood)

To relate the abstract latent state $z^i(t)$ to the observed concentration $y_{i,j}$, we define a decoding function $\text{Dec}_\psi(\cdot)$ (a neural network) that maps the latent space to the observation space. We assume that $z^i(t)$ captures all the information in the biological process such that any deviation between the true state and the observation is attributed to measurement noise. This implies that given the true trajectory $z^i(t)$, the observations are independent. This also reflects standard assumptions in pharmacokinetics, where observations $y_{i,j}$ are assumed to be conditionally independent given the subject-specific parameters [25]. The conditional likelihood of a given sequence of (rich) observations $\mathcal{R}_i = \{(t_{i,k}, y_{i,k})\}_{j=1}^{M_i}$ is therefore the product of the individual measurement likelihoods:

$$p_\psi((y_{i,j})_{j \in [1, N]} | z_0^i) = \prod_{j=1}^{M_i} p(y_{i,j} | z^i(t_{i,j})) = \prod_{j=1}^{M_i} \mathcal{N}(y_{i,j} | \text{Dec}_\psi(z^i(t_{i,j})), \sigma_{\text{obs}}^2). \quad (6)$$

3.2 Variational Inference

If we have defined the prior $p(z_0^i)$, the distribution we are really interested in is $p(z_0^i | \mathcal{O}_i, s_i)$. This distribution represents the full range of likely initial states given the observed data and covariates. However, calculating this true posterior is analytically intractable because the marginal likelihood requires integrating over the complex, non-linear dynamics defined by the Neural ODE. To overcome this, we can use Variational Inference (VI). We introduce a family of tractable distributions $q_\theta(z_0^i | \mathcal{O}_i, s_i)$ and seek the member of this family that best approximates the true posterior. Formally, we need to find the parameters θ^* that minimize a pseudo-distance (usually the Kullback-Leibler (KL) divergence) between the approximate and true posteriors:

$$\theta^* = \underset{\theta}{\operatorname{argmin}} D_{KL}\left(q_\theta(z_0^i | \mathcal{O}_i, s_i) \middle\| p(z_0^i | \mathcal{R}_i, s_i)\right). \quad (7)$$

Since the true posterior is unknown, we cannot solve this directly. Instead, we optimize the model by maximizing the Evidence Lower Bound (ELBO) [26], which is mathematically equivalent to minimizing this divergence (a classical proof is given in the Supplementary Materials).

$$\mathcal{L}_{\text{ELBO}} = \underbrace{\mathbb{E}_{z_0^i \sim q_\theta} [\log p_\psi(\mathcal{R}_i | z_0^i)]}_{\text{Reconstruction: Data Fit}} - \underbrace{D_{KL}(q_\theta(z_0^i | \mathcal{O}_i) || p(z_0^i))}_{\text{Regularization: Prior Matching}}. \quad (8)$$

The first term uses the likelihood defined in Eq. 8 to ensure that the sampled trajectory $z^i(t)$ matches the patient's sparse data points. The second term constrains the latent space to follow a prior distribution $p(z_0^i)$. While standard variational autoencoders (VAEs) assume a unimodal isotropic Gaussian prior ($\mathcal{N}(0, I)$) [26, 11], this assumption is often insufficient for clinical populations that contain distinct subgroups. To capture this heterogeneity, we employ a GMM prior with a fixed number of K components, as described in Section 3.1. This allows the model to organize the latent space into physiologically meaningful clusters in an unsupervised manner.

3.3 Deep Learning Architecture

We implement this framework using three neural network components, as illustrated in Figure 2. The key differences between Latent Neural-ODE model [11] and our method lie in the covariate encoding (described in section 3.4.1) and in the GMM prior as described in the previous section.

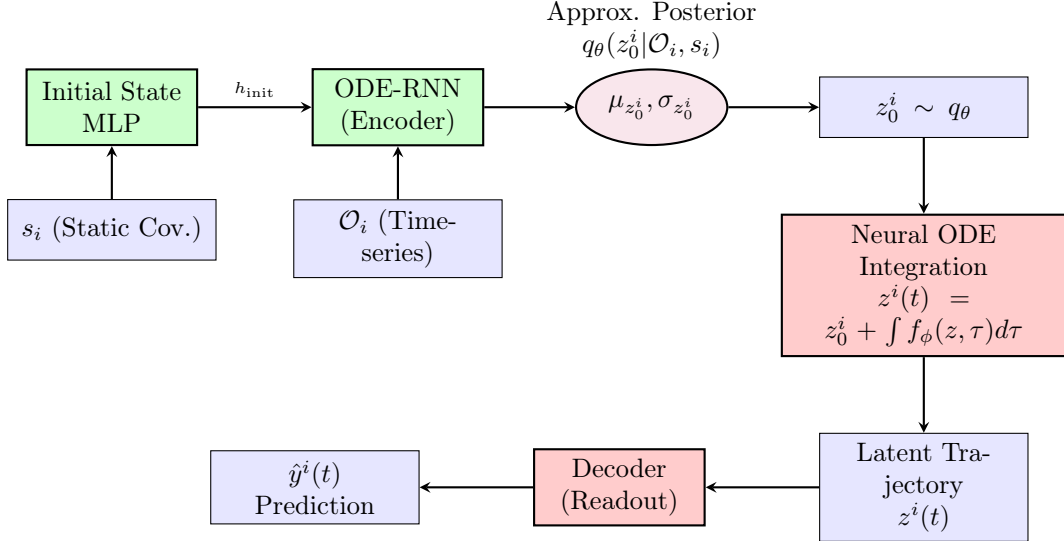


Figure 2: Schematic of the Latent ODE model architecture. The model is organized into two main blocks: the Encoder Network (green), which maps sparse clinical data to the probabilistic latent state z_0^i ; and the Generative Model (red), which solves the forward problem by integrating the learned dynamics and projecting the continuous state back to the observation space.

The Encoder: $q_\theta(z_0^i | \mathcal{O}_i, s_i)$

The encoder maps the clinical data into a probabilistic latent space. To accommodate both static covariates (e.g., genotype) and irregularly sampled time-series data (e.g., drug concentration), we employ a hybrid architecture consisting of: (i) a *Covariate Encoding*, in which a Multilayer Perceptron (MLP) [27] processes s_i to initialize the hidden state of the recurrent network; and (ii) a *Temporal Encoding*, in which an ODE-RNN [11] reads the sparse observations \mathcal{O}_i backward in time. This specialized recurrent architecture naturally handles irregular time intervals. The final output is the mean μ and variance σ of the Gaussian posterior $q_\theta(z_0^i)$, from which we sample the patient’s initial biological state z_0^i .

The Generator: Latent Dynamics and decoder

Once we obtain the initial state z_0^i , we need to describe its evolution over time. This is where the Neural ODE replaces the standard pharmacokinetic equations. We define the time derivative of the latent state as a neural network f_ϕ , as described in Eq. 4. By integrating this equation with a numerical solver (e.g., Dormand–Prince or Runge–Kutta method [28]), we obtain the continuous latent trajectory $z^i(t)$. Importantly, f_ϕ is not pre-defined; instead, the model learns the drug dynamics directly from the data.

Finally, a linear decoder projects this abstract state back to the observation space at any desired time point to produce the concentration estimate $\hat{y}^i(t)$.

4 Experiments

The performance of the proposed model was assessed through both simulation studies and an application to real-world data. Two independent datasets were used for the real-data case study, while the simulation study was designed to mirror the characteristics of the real-data setting. In the real-data analysis, the proposed model was compared with two existing methods, whereas in the simulation study it was compared with one of these methods.

4.1 Datasets

Two independent retrospective clinical datasets of tacrolimus pharmacokinetics in renal transplant recipients were used. The first dataset, hereafter referred to as the Development Dataset, comprised $N = 178$ full PK profiles and was used for model training and internal validation. The second dataset, hereafter referred to as the External Dataset, comprised $N = 75$ full PK profiles that were completely unseen during model development and originated from the study by Marquet et al. (2018) [29]. This dataset was used exclusively to assess model generalizability.

Consistent with the notation defined in Section 3, each patient i in these datasets provides a rich sampling profile $\mathcal{R}_i = \{(t_{i,k}, y_{i,k})\}_{k=1}^{M_i}$. Each profile contains between $M_i = 10$ and 12 samples, corresponding to the rich sampling schemes collected at approximately 0, 0.33, 0.67, 1, 2, 3, 4, 6, 8, 12, and 24 hours. For the purpose of AUC prediction from limited data, the model input \mathcal{O}_i is a sparse subset of \mathcal{R}_i consisting of only $m_i = 3$ observations. Following standard clinical limited sampling strategies, we selected the measurements at $t \in \{0, 1, 3\}$ hours to form \mathcal{O}_i . The static covariate vector s_i includes the CYP3A5 genotype (binary variable), administered dose d_i , and formulation.

4.2 Simulation data generation

We designed a controlled simulation study to evaluate the Latent ODE against standard methods (NLME based) in scenarios where the “ground truth” data-generating process is perfectly known. We generated synthetic data using a structural PK model that mathematically mimics how tacrolimus concentration changes in human body [13]. At a high level, this model represents the body as a system of interconnected reservoirs (blood and organs), referred to as compartments: (i) **Absorption**, in which the delay between oral administration and appearance in the systemic circulation is modeled using a chain of “transit” compartments; (ii) **Distribution**, where the drug flows between the central compartment (blood) and peripheral compartments (organs), governed by the central and peripheral volumes of distribution (V_c, V_p) and the inter-compartmental clearance (Q); and (iii) **Elimination**, in which the drug is removed from the body at a rate characterized by the clearance parameter (CL). To generate a realistic population, inter-individual variability was introduced by assuming log-normal distributions for the model parameters (commonly referred to as random effects). Known biological influences were also incorporated, including the effect of genotype on elimination clearance (CL) and the impact of formulation type (immediate- vs. extended-release) on absorption. A combined proportional and additive residual error model was applied to the simulated concentrations to account for measurement error. Full mathematical details are provided in the Supplementary Materials.

The study examined three distinct scenarios. The first scenario, hereafter referred to as Correct Model Specification scenario, simulated data from the exact structural model just described and also used by the NLME comparator method [13]. The second scenario, hereafter referred to as Unaccounted Covariate Effect scenario, introduced a misspecification where drug clearance depended on an unobserved covariate (Hematocrit). Finally, the Non-Linear Elimination Kinetics scenario simulated data using saturable Michaelis-Menten elimination rather than the linear first-order elimination assumed by the previous model. The workflow for these simulations is depicted in Figure 3 and visualization is available in Supplementary Materials (Figure 8). The

true patient’s AUC, with $t^* = 24$ h in Eq. 2, was calculated from the simulated noiseless, densely sampled concentration-time trajectory (time resolution: 0.1 hours) using the trapezoidal rule.

4.3 Architecture configuration

We implemented the model using a latent state dimension of $D = 10$. The prior over the initial state z_0 was modeled as a Gaussian Mixture Model with $K = 4$ components. For the inference network, we utilized an ODE-RNN encoder where the recurrent component was a GRU with 100 hidden units, and the continuous dynamics between observations were integrated using the Euler method. The generative latent dynamics function f_ϕ was parameterized by a neural network with one hidden layer of 100 units and Tanh activations. We solved the generative initial value problem using the Dormand-Prince (dopri5) adaptive step-size solver, while the decoder was defined as a linear projection mapping the latent state directly to the observation space.

4.4 Competing methods setting

For the Latent ODE, patient’s AUC were derived by generating a dense concentration trajectory (time resolution: 0.1 hours) from the predicted latent state, which was then integrated using the trapezoidal rule.

To evaluate our model, we compared it against two baselines. Both rely on the NLME framework but utilize different estimation strategies as described Section 2.1. The first one, ISBA, is the ABIS/ISBA estimator (<https://abis.chu-limoges.fr/>). ISBA uses pharmacokinetic model (NLME) combined with the Iterative Two-Stage (IT2B) estimation method [19]. The second one was MAP-BE_{SAEM}, a classic NLME model based on the work of Woillard et al. (2011) [13], which we fitted on our entire development dataset using the SAEM algorithm implemented in Monolix [30]. This second benchmark was used in the external validation stage to ensure a direct and fair comparison of generalization. In our comparison, the two methods derived the AUC directly from the estimated individual posterior parameters. For the second one, the curve was simulated using the estimated parameters and integrated numerically using Monolix.

4.4.1 Metrics

Model performance was evaluated using the Root Mean Squared Percentage Error (RMSPE) for precision and the Mean Percentage Error (MPE) for bias. Let $AUC_{ref,i}$ be the ground truth area under the curve (between $t = 0$ and $t = t^*$) for patient i and \widehat{AUC}_i be the predicted value. The metrics are defined as follows:

$$RMSPE = \sqrt{\frac{1}{N} \sum_{i=1}^N \left(\frac{\widehat{AUC}_i - AUC_{ref,i}}{AUC_{ref,i}} \right)^2} \times 100 \quad (9)$$

$$MPE = \frac{1}{N} \sum_{i=1}^N \left(\frac{\widehat{AUC}_i - AUC_{ref,i}}{AUC_{ref,i}} \right) \times 100 \quad (10)$$

4.4.2 Simulation setting

As summarized in Figure 3, for each scenario, 100 simulation runs were generated. Each run consisted of a dataset of 1,000 patients, which was split into 200 patients for training and 800 patients for testing. The proposed model was compared with the MAP-BE_{SAEM} approach.

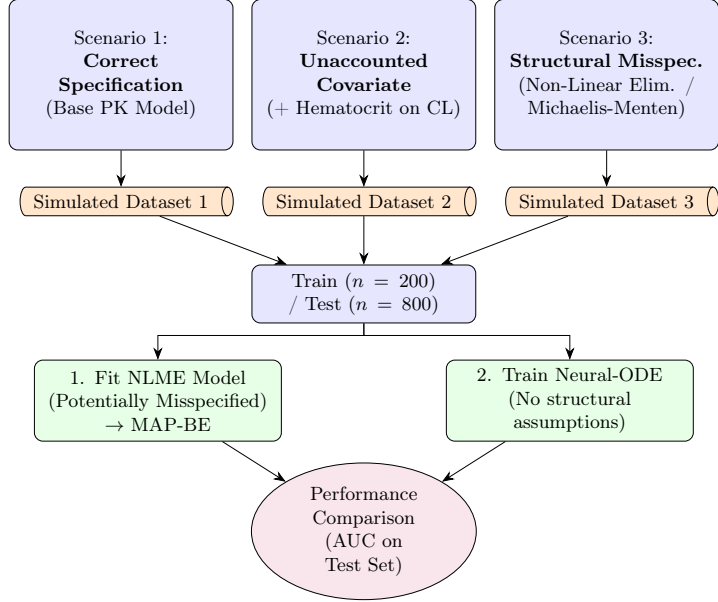


Figure 3: Workflow for the three-scenario simulation study. Each scenario generates a unique dataset to test the models under different conditions.

4.4.3 Validation on Clinical Data

We performed a two-stage validation on the real-world clinical datasets. The first stage, Internal Validation, assessed learning capacity through a repeated random sub-sampling cross-validation on the development dataset. In each of 50 iterations, a new Latent ODE model was trained on a random 80% of the data and evaluated on the held-out 20%, with its performance compared directly to the $it2B_{ISBA}$ estimator on the same test set. The second stage, External Validation, assessed generalizability. For this, a final Latent ODE model was trained on the entire development dataset and evaluated on the completely unseen external dataset [29], and its performance was compared against both $it2B_{ISBA}$ and $MAP-BE_{SAEM}$.

5 Results

5.1 Model Robustness on Simulated Data

Table 1 presents the results in terms of bias and RMSPE across the three simulated scenarios. In Scenario 1 (Correct Model Specification), where the data perfectly matched the $MAP-BE_{SAEM}$ assumptions, the Latent ODE achieved a predictive performance comparable to the $MAP-BE_{SAEM}$, demonstrating its ability to learn the correct dynamics even on its competitor’s “home ground.” In Scenario 2 (Unaccounted Covariate) and Scenario 3 (Non-Linear Elimination), which introduced model misspecification and violated the $MAP-BE_{SAEM}$ core assumptions, the Latent ODE demonstrated greater robustness. Its flexible, data-driven nature allowed it to adapt to the unobserved sources of variability or structural changes, resulting in a lower prediction error compared to the traditional model.

5.2 Performance on Real-World Clinical Data

5.2.1 Internal Validation

Across the 50-folds cross-validation study, the Latent ODE model yielded consistently and significantly more accurate predictions than the state-of-the-art $it2B_{ISBA}$ estimator. The mean performance metrics, shown in Table 2, reveal a 1.2 percentage point improvement in precision

Table 1: Performance comparison (Bias and Precision) across simulation scenarios. Statistical significance (Sig.) is based on a paired t-test [31] between the two model distributions (100 simulations by scenario were performed).

Scenario	Metric	Latent ODE (Proposed)	MAP-BE (Competitor)	Sig.
Scenario 1: Correct Spec.	MPE (%)	0.0123 ± 0.0210	0.0106 ± 0.0166	n.s.
	RMSPE (%)	16.72 ± 1.14	16.63 ± 1.23	n.s.
Scenario 2: Unaccounted Cov.	MPE (%)	0.0036 ± 0.0252	0.0235 ± 0.0147	*
	RMSPE (%)	20.42 ± 1.19	22.96 ± 0.73	*
Scenario 3: Structural Misspec.	MPE (%)	0.0039 ± 0.0246	0.0102 ± 0.0749	n.s.
	RMSPE (%)	15.40 ± 0.04	23.57 ± 8.55	*

* indicates statistical significance ($p \leq 0.0001$); n.s. = not significant.

(RMSPE) and substantially lower bias (MPE). A paired t-test confirmed this improvement was statistically significant for both metrics ($p < 0.001$). This consistent outperformance is visualized in Figure 4.

Table 2: Mean performance from 50 runs of 80/20 cross-validation on the development dataset.

Method	Mean RMSPE (%) \pm SD	Mean MPE (%) \pm SD
Latent ODE	$7.99\% \pm 1.60\%$	$1.11\% \pm 1.72\%$
it2B _{ISBA}	$9.24\% \pm 1.27\%$	$4.74\% \pm 1.35\%$

5.2.2 External Validation for Generalizability

The final Latent ODE model, trained on the full development dataset, demonstrated strong generalizability to the unseen external data. As shown in Table 3, it achieved an RMSPE of 10.82%, a performance comparable to both the state-of-the-art it2B_{ISBA} (11.58%) and the MAP-BE_{SAEM} model fitted on the identical development data (11.48%). This confirms that the data-driven model can learn a representation of tacrolimus dynamics that is as robust as traditional, expert-defined pharmacokinetics models.

Table 3: Performance on the external dataset ($n = 75$).

Prediction Method	RMSPE (%) [Precision]	MPE (%) [Bias]
Latent ODE (trained on development set)	10.82%	+3.47%
it2B _{ISBA} (Clinically used model)	11.58%	-2.91%
MAP-BE _{SAEM} (fitted on development set)	11.48%	-2.28%

5.3 Model interpretability through the latent space

While neural networks are often criticized for their “black box” nature, the Latent ODE architecture used in this study offers distinct advantages for interpretation. Firstly, the model generates a full, continuous concentration-time curve, which allows for qualitative assessment by a clinical expert. Furthermore, the model’s internal latent space, z_0^i , provides a powerful second avenue for interpretation. The VAE framework regularizes this space, encouraging an organized representation. To visualize this, we applied Principal Component Analysis (PCA) and t-Distributed

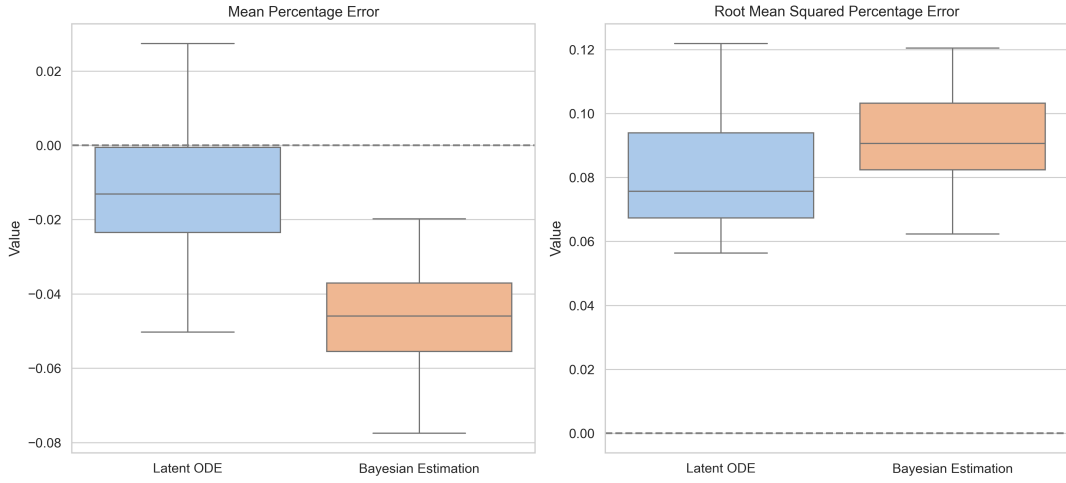


Figure 4: Distribution of performance metrics over 50 cross-validation runs. The Latent ODE (blue) shows consistently better precision (lower RMSPE) and less bias (MPE closer to zero) than the it2B benchmark (orange).

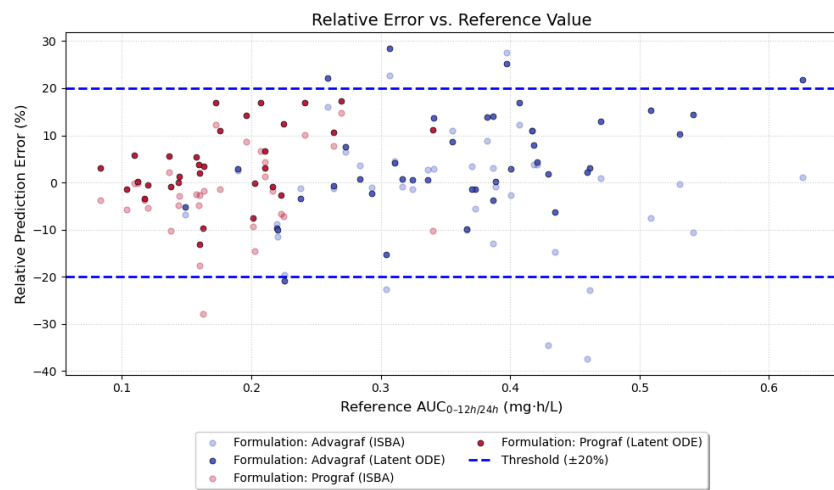


Figure 5: Relative prediction error versus the reference AUC value on the external dataset for the Latent ODE model (dark colors) and the ISBA competitor (light colors). Categories correspond to the two kinds of formulation in the dataset

Stochastic Neighbor Embedding (t-SNE) to the latent space embeddings (z_0) of the external validation cohort. As shown in Figure 6, the latent space exhibits a clear, physiologically meaningful organization. Panels (a) and (b) show a distinct separation of patients based on their CYP3A5 genotype (expresser vs. non-expresser), while panels (c) and (d) show separation based on treatment formulation (Once-A-Day vs. Twice-A-Day). These are two of the most significant determinants of tacrolimus pharmacokinetics, and the model has learned to map them to different regions of the latent space without being explicitly instructed to do so. Moreover, Panels (e) and (f) show that the administered dose is represented as a smooth gradient. This structured internal representation confirms that the model is learning key pharmacokinetic relationships from the data, which increases confidence in its predictions and provides a valuable tool for exploring patient heterogeneity. This latent space can also be used to generate new, synthetic patient profiles by sampling from the learned distribution.

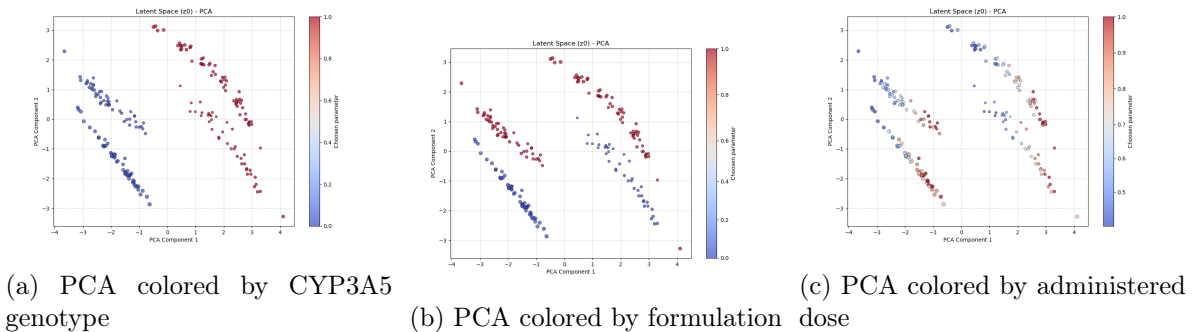


Figure 6: Visualization of the latent space (z_0) for the external validation set using PCA. Left part shows patient separation by CYP3A5 genotype, central part by formulation and left part by administered dose. The clear organization demonstrates a physiologically meaningful learned representation and justify a posteriori the use of GMM as prior.

5.4 Model Parsimony and Data Requirements

A key consideration for ML models is the balance between flexibility and complexity. Our Neural-ODE framework allows for a parsimonious design. The three parts of the network (encoder, dynamics, decoder) are intentionally shallow to remain usable without massive datasets. We tested this parsimony experimentally: we found that, on real data, even with a training set as small as 25 patients, the model achieved decent results, as shown in Table 4.

This efficient design also results in a computationally light model. Training on 80% (141 patients) of the development dataset required less than 6 minutes on a standard consumer-grade CPU, demonstrating a workflow no more demanding than developing a conventional NLME model.

Table 4: Performance evolution by increasing train set size. Uncertainty computed on 100 training runs. All training were performed on the Development Dataset

Size of train set	RMSPE (%) [Precision]	MPE (%) [Bias]
25 Patients	$13.55\% \pm 2.35\%$	$0.72\% \pm 1.65\%$
50 Patients	$11.35\% \pm 0.97\%$	$1.42\% \pm 1.39\%$
100 Patients	$10.25\% \pm 1.00\%$	$0.2\% \pm 1.26\%$
141 Patients	$8.75\% \pm 1.00\%$	$0.2\% \pm 1.26\%$

6 Discussion

This study provides a rigorous evaluation of a Latent ODE model for tacrolimus AUC prediction, comparing it against traditional, fixed-structure NLME methods. Our findings, beginning with a foundational simulation study, demonstrate that this flexible, data-driven approach is not only a viable alternative but also exhibits superior robustness under the kinds of model misspecification observable in real-world clinical scenarios.

The simulation study was designed to probe the theoretical advantages and limitations of both modeling philosophies. In the first scenario, a “best-case” for the traditional approach where the data perfectly matched the structural and statistical assumptions of the NLME model, we found no evidence that the classic MAP-BE method was superior. The Latent ODE achieved a comparable performance, demonstrating that its flexible architecture does not incur a penalty even when a simpler, correctly specified model exists. In this scenario where the model that generates the data has exactly the same structure as the predictive one, we cannot hope to do better than even performance.

However, the subsequent scenarios revealed the critical advantage of the data-driven approach. When an influential covariate (hematocrit) was omitted from the test set, the performance of the assumption-reliant NLME model dropped significantly. The Latent ODE, having learned a more holistic representation of patient dynamics, was more resilient to this missing information.

Similarly, in Scenario 3, when the drug elimination mechanism was changed from linear (first-order) to saturable (Michaelis-Menten) kinetics the performance of the NLME model degraded. The MAP-BE estimator, constrained by its rigid structural equation, attempted to fit the saturable data with a linear model, leading to bias. Conversely, the assumption-free Latent ODE successfully learned the non-linear trajectory directly from the sparse data, providing robust predictions even when the underlying biological mechanism deviated from standard assumptions.

These insights from our controlled simulations provide an essential context for interpreting the model’s performance on the more complex and noisy real-world clinical datasets. As described in the dataset section, we encounter a case where the original NLME model was developed with a specific covariate (Hematocrit) available at the time, but these data are no longer available in the test set. This case is precisely what Scenario 2 mimics, showing that the scenarios chosen are common real-world clinical scenarios. Having established the Latent ODE’s resilience to misspecification, we then validated its practical utility. In the internal cross-validation, the model demonstrated a strong capacity to learn from in-distribution data, achieving a high degree of precision and yielding consistently and significantly lower prediction errors than the it2B benchmark. Furthermore, the external validation confirmed that the Latent ODE—without any pre-specified structural constraints—successfully learned a representation of tacrolimus dynamics that was as robust and generalizable as a traditional, expert-defined pharmacokinetic model.

6.1 A Framework for More Complex Modeling

We argue that the most significant contribution of this work is the demonstration of a flexible and extensible framework for dynamic modeling. While traditional NLME models are powerful, incorporating diverse data types can be challenging. Our Neural-ODE architecture, however, is inherently modular. A key example is our encoder’s initialization step, where static covariates are used to define the initial patient state ($h_{initial}$). This simple MLP could easily be replaced by more sophisticated neural network architectures to integrate complex, high-dimensional data. One could, for instance, use this framework to condition pharmacokinetic dynamics on genomic data, gene expression profiles, or even medical imaging features—modalities that are difficult to mechanistically link within the rigid structure of conventional PopPK models. This positions the Neural-ODE as a new tool for AUC prediction, but also as a new method for building new multi-modal models in personalized medicine.

6.2 Open Source Contribution

A significant barrier to the adoption of advanced machine learning models in pharmacokinetic is the lack of accessible code. To address this, we have made our full implementation publicly available at <https://github.com/BenJMaurel/PharmaNODE>. This includes the Latent ODE training pipeline, the pre-trained models used in our external validation, and the simulation environments. We hope this open-source contribution will facilitate reproducibility and allow the pharmacokinetic community to adapt this flexible architecture to other drugs and therapeutic areas.

6.3 Limitations

This study has some limitations. Firstly, the data-driven nature of the Neural-ODE comes at the cost of direct mechanistic interpretability. The model was developed on a specific population of renal transplant recipients and only has the generalizability power of its training distribution. Lastly, as with any data-driven model, the quality of the model highly depends on the quality of the data. Errors are common in healthcare datasets, and if they cannot be corrected or filtered before training, the model will inevitably suffer from the classic garbage in, garbage out effect, degrading its overall quality.

While the Neural Latent ODE approach demonstrated a statistically superior predictive performance, we must acknowledge that this statistical significance does not strictly translate into clinical significance. In the daily practice of MIPD, a marginal gain in precision of less than 1% is unlikely to modify dosage adjustments, as it falls well within the ranges of analytical uncertainty and intra-individual variability. However, the primary value of introducing Neural ODEs lies beyond the immediate reduction of AUC estimation error. Unlike traditional parametric approaches constrained by rigid structural assumptions, this continuous-depth framework offers the necessary plasticity to model complex, irregular dynamics. Consequently, these results should be viewed as a proof of concept; they pave the way for addressing far more intricate challenges, such as the seamless integration of high-dimensional multimodal data and the transition from simple pharmacokinetic exposure estimation to the direct prediction of pharmacodynamic endpoints and long-term clinical outcomes

7 Conclusion

This study establishes the Neural-ODE as a viable and powerful tool for AUC -guided MIPD of tacrolimus. By demonstrating predictive accuracy comparable to gold-standard MAP-BE methods in both internal and external validation, our work provides strong evidence for its reliability in a standard clinical scenario. The primary advantage of the Neural-ODE, however, does not lie in marginally improving precision for this specific problem, but in its inherent flexibility. Its ability to learn individual dynamics without pre-specified structural assumptions provides a promising and extensible foundation for the new pharmacokinetic tools. As clinical data becomes increasingly multi-modal, such data-driven frameworks will be essential for advancing the frontier of personalized medicine.

CRediT authorship contribution statement

Benjamin Maurel: Writing – original draft, Methodology, Formal analysis, Visualization, Software, Validation. Agathe Guilloux: Writing – review and editing, Methodology. Sarah Zohar: Writing – review and editing. Moreno Ursino: Writing – review and editing, Conceptualization, Supervision. Jean-Baptiste Woillard: Writing – review and editing, Conceptualization, Funding acquisition.

References

- [1] Mercè Brunet, Teun Van Gelder, Anders Åsberg, Vincent Haufroid, Dennis A Hesselink, Loralie Langman, Florian Lemaitre, Pierre Marquet, Christoph Seger, Maria Shipkova, et al. Therapeutic drug monitoring of tacrolimus-personalized therapy: second consensus report. *Therapeutic drug monitoring*, 41(3):261–307, 2019.
- [2] Lien Haverals, Laurence Roosens, Kristien Wouters, Pierre Marquet, Caroline Monchaud, Annick Massart, Daniel Abramowicz, and Rachel Hellemans. Does the tacrolimus trough level adequately predict drug exposure in patients requiring a high tacrolimus dose? *Transplantation Direct*, 9(4):e1439, 2023.
- [3] Lewis B Sheiner and Stuart L Beal. Bayesian individualization of pharmacokinetics: simple implementation and comparison with non-Bayesian methods. *Journal of pharmaceutical sciences*, 71(12):1344–1348, 1982.
- [4] Wei Zhao, May Fakhoury, Véronique Baudouin, Anne Maisin, Georges Deschênes, and Evelyne Jacqz-Aigrain. Limited sampling strategy for estimating individual exposure of tacrolimus in pediatric kidney transplant patients. *Therapeutic drug monitoring*, 33(6):681–687, 2011.
- [5] Marie Davidian and David M Giltinan. *Nonlinear models for repeated measurement data*. Routledge, 2017.
- [6] Lewis B Sheiner, Stuart Beal, Barr Rosenberg, and Vinay V Marathe. Forecasting individual pharmacokinetics. *Clinical Pharmacology & Therapeutics*, 26(3):294–305, 1979.
- [7] Ene I Ette and Paul J Williams. Population pharmacokinetics I: background, concepts, and models. *Annals of Pharmacotherapy*, 38(10):1702–1706, 2004.
- [8] José Miguel Laínez, Gary Blau, Linas Mockus, Seza Orçun, and Gintaras V Reklaitis. Pharmacokinetic based design of individualized dosage regimens using a Bayesian approach. *Industrial & Engineering Chemistry Research*, 50(9):5114–5130, 2011.
- [9] Sebastian Greppmair, Alexander Brinkmann, Anka Roehr, Otto Frey, Stefan Hagel, Christoph Dorn, Amélie Marsot, Ibrahim El-Haffaf, Michael Zoller, Thomas Saller, et al. Towards model-informed precision dosing of piperacillin: multicenter systematic external evaluation of pharmacokinetic models in critically ill adults with a focus on Bayesian forecasting. *Intensive Care Medicine*, 49(8):966–976, 2023.
- [10] Ricky TQ Chen, Yulia Rubanova, Jesse Bettencourt, and David K Duvenaud. Neural ordinary differential equations. *Advances in neural information processing systems*, 31, 2018.
- [11] Yulia Rubanova, Ricky TQ Chen, and David K Duvenaud. Latent ordinary differential equations for irregularly-sampled time series. *Advances in neural information processing systems*, 32, 2019.
- [12] Bernd Meibohm and Hartmut Derendorf. Basic concepts of pharmacokinetic/pharmacodynamic (PK/PD) modelling. *International journal of clinical pharmacology and therapeutics*, 35(10):401–413, 1997.
- [13] Jean-Baptiste Woillard, Brenda CM de Winter, Nassim Kamar, Pierre Marquet, Lionel Rostaing, and Annick Rousseau. Population pharmacokinetic model and Bayesian estimator for two tacrolimus formulations—twice daily Prograf® and once daily Advagraf®. *British journal of clinical pharmacology*, 71(3):391–402, 2011.

[14] Charles C Margossian, Yi Zhang, and William R Gillespie. Flexible and efficient Bayesian pharmacometrics modeling using Stan and Torsten, part I. *CPT: Pharmacometrics & Systems Pharmacology*, 11(9):1151–1169, 2022.

[15] Thanh Bach and Guohua An. Comparing the performance of first-order conditional estimation (FOCE) and different expectation–maximization (EM) methods in NONMEM: real data experience with complex nonlinear parent-metabolite pharmacokinetic model. *Journal of pharmacokinetics and pharmacodynamics*, 48(4):581–595, 2021.

[16] Bernard Delyon, Marc Lavielle, and Eric Moulines. Convergence of a stochastic approximation version of the EM algorithm. *Annals of statistics*, pages 94–128, 1999.

[17] Yann Merlé and France Mentré. Bayesian design criteria: computation, comparison, and application to a pharmacokinetic and a pharmacodynamic model. *Journal of pharmacokinetics and biopharmaceutics*, 23(1):101–125, 1995.

[18] Radojka M Savic and Mats O Karlsson. Importance of shrinkage in empirical bayes estimates for diagnostics: problems and solutions. *The AAPS journal*, 11(3):558–569, 2009.

[19] Franck Saint-Marcoux, Jean-Baptiste Woillard, Camille Jurado, and Pierre Marquet. Lessons from routine dose adjustment of tacrolimus in renal transplant patients based on global exposure. *Therapeutic Drug Monitoring*, 35:322–7, 2013.

[20] Jean-Baptiste Woillard, Marc Labriffe, Jean Debord, and Pierre Marquet. Tacrolimus exposure prediction using machine learning. *Clinical Pharmacology & Therapeutics*, 110(2):361–369, 2021.

[21] James Lu, Kaiwen Deng, Xinyuan Zhang, Gengbo Liu, and Yuanfang Guan. Neural-ode for pharmacokinetics modeling and its advantage to alternative machine learning models in predicting new dosing regimens. *Iscience*, 24(7), 2021.

[22] Dominic Stefan Bräm, Uri Nahum, Johannes Schropp, Marc Pfister, and Gilbert Koch. Low-dimensional neural odes and their application in pharmacokinetics. *Journal of Pharmacokinetics and Pharmacodynamics*, 51(2):123–140, 2024.

[23] Tommaso Giacometti, Ettore Rocchi, Pier Giorgio Cojutti, Federico Magnani, Daniel Remondini, Federico Pea, and Gastone Castellani. Leveraging neural odes for population pharmacokinetics of dalbavancin in sparse clinical data. *Entropy*, 27(6):602, 2025.

[24] Scott M Lundberg and Su-In Lee. A unified approach to interpreting model predictions. *Advances in neural information processing systems*, 30, 2017.

[25] Cécile Proust-Lima, Viviane Philipps, and Benoit Liquet. Estimation of extended mixed models using latent classes and latent processes: the R package lcmm. *Journal of statistical software*, 78:1–56, 2017.

[26] Diederik P Kingma and Max Welling. Auto-encoding variational bayes. *arXiv preprint arXiv:1312.6114*, 2013.

[27] Ian Goodfellow, Yoshua Bengio, Aaron Courville, and Yoshua Bengio. *Deep learning*, volume 1. MIT press Cambridge, 2016.

[28] John R Dormand and Peter J Prince. A family of embedded Runge-Kutta formulae. *Journal of computational and applied mathematics*, 6(1):19–26, 1980.

- [29] Pierre Marquet, Laetitia Albano, Jean-Baptiste Woillard, Lionel Rostaing, Nassim Kammar, Charlotte Sakarovitch, Philippe Gatault, Matthias Buchler, Bernard Charpentier, Eric Thervet, et al. Comparative clinical trial of the variability factors of the exposure indices used for the drug monitoring of two tacrolimus formulations in kidney transplant recipients. *Pharmacological Research*, 129:84–94, 2018.
- [30] Lixoft SAS. Monolix version 2024r1, 2024.
- [31] Henry Hsu and Peter A Lachenbruch. Paired t test. *Wiley StatsRef: statistics reference online*, 2014.

Supplementary Materials

8 General Mathematical Formulation of NLME

For a subject i , the observed drug concentration y_{ij} at time t_{ij} is modeled as:

$$y_{ij} = m_{\text{struct}}(t_{ij}, \psi_i) + g(t_{ij}, \psi_i) \cdot \varepsilon_{ij}, \quad \varepsilon_{ij} \sim \mathcal{N}(0, \sigma^2). \quad (11)$$

where $m_{\text{struct}}(\cdot)$ is the structural model (e.g., compartmental differential equations), $g(\cdot)$ is the residual error model, and ψ_i represents the vector of individual pharmacokinetic parameters. These parameters are defined by typical population values θ_{pop} and individual random effects $\eta_i \sim \mathcal{N}(0, \Omega)$ such that $\psi_i = h(\theta_{\text{pop}}, s_i, \eta_i)$, where s_i denotes static covariates.

The Maximum A Posteriori Bayesian Estimator (MAP-BE) finds the mode of the posterior distribution of η_i :

$$\hat{\eta}_{\text{MAP}} = \underset{\eta_i}{\operatorname{argmin}} \left[\sum_{j=1}^{n_i} \frac{(y_{ij} - m_{\text{struct}}(t_{ij}, \psi_i))^2}{g(t_{ij}, \psi_i)^2 \sigma^2} + \eta_i^T \Omega^{-1} \eta_i \right]. \quad (12)$$

9 The Structural PK Model

The model describes drug disposition using a system of first-order Ordinary Differential Equations (ODEs). The structure includes four sequential transit compartments for absorption ($A_{\text{Trans},1}$ to $A_{\text{Trans},4}$), a central compartment (A_c), and a peripheral compartment (A_p).

9.1 System of Ordinary Differential Equations (Linear)

The amount of drug (mg) in each compartment over time t (hours) is given by:

$$\begin{aligned} \frac{dA_{\text{Trans},1}}{dt} &= -K_{tr} \cdot A_{\text{Trans},1} \\ \frac{dA_{\text{Trans},i}}{dt} &= K_{tr} \cdot A_{\text{Trans},i-1} - K_{tr} \cdot A_{\text{Trans},i} \quad \text{for } i \in \{2, 3, 4\} \\ \frac{dA_c}{dt} &= K_{tr} \cdot A_{\text{Trans},4} - (k_{10} + k_{12}) \cdot A_c + k_{21} \cdot A_p \\ \frac{dA_p}{dt} &= k_{12} \cdot A_c - k_{21} \cdot A_p \end{aligned}$$

The micro-rate constants are derived from the primary PK parameters (CL, V_c, Q, V_p) as follows:

$$k_{\text{elim}} = \frac{CL}{V_c}, \quad k_{12} = \frac{Q}{V_c}, \quad k_{21} = \frac{Q}{V_p}$$

The model output is the drug concentration in the central compartment (C_c) in ng/mL:

$$C_c(t) = \frac{A_c(t)}{V_c} \cdot 1000$$

10 The Statistical Model

A Nonlinear Mixed-Effects (NLME) framework is used to describe parameter variability.

10.1 Covariate Model

The typical value (TV) of a parameter is adjusted for covariates. The relationships are:

$$\begin{aligned}\log(K_{tr,i}) &= \log(\theta_{K_{tr}}) + \theta_{ST}^{K_{tr}} \cdot ST_i + \eta_{K_{tr},i} \\ \log(CL_i) &= \log(\theta_{CL}) + \theta_{CYP}^{CL} \cdot CYP_i + \eta_{CL,i} \\ \log(V_{c,i}) &= \log(\theta_{V_c}) + \theta_{ST}^{V_c} \cdot ST_i + \eta_{V_c,i} \\ \log(Q_i) &= \log(\theta_Q) + \eta_{Q,i} \\ \log(V_{p,i}) &= \log(\theta_{V_p}) + \eta_{V_p,i}\end{aligned}$$

Where ST_i is 1 for the Prograf formulation and CYP is 1 for CYP3A5 expressers (0 else). The random effects are normally distributed with a mean of zero:

- IPV: $\eta_i \sim \mathcal{N}(0, \omega^2)$

A combined proportional and additive error model relates the observed ($Y(t)$) and predicted ($C_c(t)$) concentrations:

$$Y(t) = C_c(t) \cdot (1 + \varepsilon_{\text{prop},ij}) + \varepsilon_{\text{add},ij}$$

The residual error terms are normally distributed with a mean of zero:

- Proportional error: $\varepsilon_{\text{prop}} \sim \mathcal{N}(0, \sigma_{\text{prop}}^2)$
- Additive error: $\varepsilon_{\text{add}} \sim \mathcal{N}(0, \sigma_{\text{add}}^2)$

11 Model Parameters

Table 5: Population Mean Parameters (θ).

Parameter	Value	Description
$\theta_{K_{tr}}$	3.34	Base absorption rate constant (h^{-1})
θ_{CL}	21.2	Base apparent clearance (L/h)
$\theta_{ST}^{K_{tr}}$	1.53	Multiplier for K_{tr} for Prograf
θ_{HCT}	-1.14	Exponent for hematocrit effect on CL
θ_{CYP}^{CL}	2.00	Multiplier for CL for CYP3A5 expressers
θ_{V_c}	486.0	Base apparent central volume (L)
$\theta_{ST}^{V_c}$	0.29	Multiplier for V_c for Prograf
θ_Q	79.0	Apparent inter-compartmental clearance (L/h)
θ_{V_p}	271.0	Apparent peripheral volume (L)

Table 6: Standard Deviations of Random Effects.

Parameter	IPV (ω)
K_{tr}	0.24
CL	0.28
Q	0.54
V_c	0.31
V_p	0.60

Table 7: Standard Deviations of Residual Error.

Parameter	Value	Description
σ_{prop}	0.113	Prop. error SD
σ_{add}	0.71	Add. error SD

11.1 Scenario 2

The model is updated to :

$$\log(CL_i) = \log(\theta_{CL}) + \theta_{CYP}^{CL} \cdot CYP_i + \theta_{HCT} \cdot \log\left(\frac{HT_i}{35}\right) + \eta_{CL,i}$$

11.2 Scenario 3: Non-Linear Elimination

In this scenario, the linear elimination term is replaced by Michaelis-Menten kinetics. The ODE for the central compartment becomes:

$$\frac{dA_c}{dt} = K_{tr} \cdot A_{Trans,4} - \frac{V_{max} \cdot C_c}{K_m + C_c} - k_{12} \cdot A_c + k_{21} \cdot A_p$$

where $C_c = A_c/V_c$

The linear clearance parameter CL is replaced by V_{max} (maximum elimination rate) and K_m (Michaelis constant).

S2. Prediction Figures

12 Tacrolimus Formulations and AUC Targets

In this study, we utilize data from renal transplant recipients receiving two distinct formulations of tacrolimus. Although both formulations contain the same active moiety, their release profiles and dosing schedules differ, necessitating different definitions for the Area Under the Curve (AUC) target.

1. Immediate-Release Formulation (Prograf)

- **Description:** This is the standard immediate-release capsule formulation of tacrolimus.
- **Dosing Regimen:** It is administered twice daily (BID), typically every 12 hours (e.g., 8:00 AM and 8:00 PM).
- **AUC Definition:** For patients on this formulation, the therapeutic exposure is quantified over the 12-hour dosing interval. Thus, the target variable is AUC_{0-12h} .

2. Extended-Release Formulation (Advagraf)

- **Description:** This is a prolonged-release formulation designed to release the drug more slowly over time to allow for once-daily administration.
- **Dosing Regimen:** It is administered once daily (QD), typically in the morning (every 24 hours).
- **AUC Definition:** For patients on this formulation, the therapeutic exposure is quantified over the full 24-hour dosing interval. Thus, the target variable is AUC_{0-24h} .

Note on Comparison: To ensure consistency when comparing model errors across the full dataset, all relative metrics (such as RMSPE and MPE) are calculated relative to the specific target AUC for that patient (AUC_{0-12h} for Prograf and AUC_{0-24h} for Advagraf).

13 Simulation Data Visualization

Figure 8 displays the ground truth concentration data generated for each scenario.

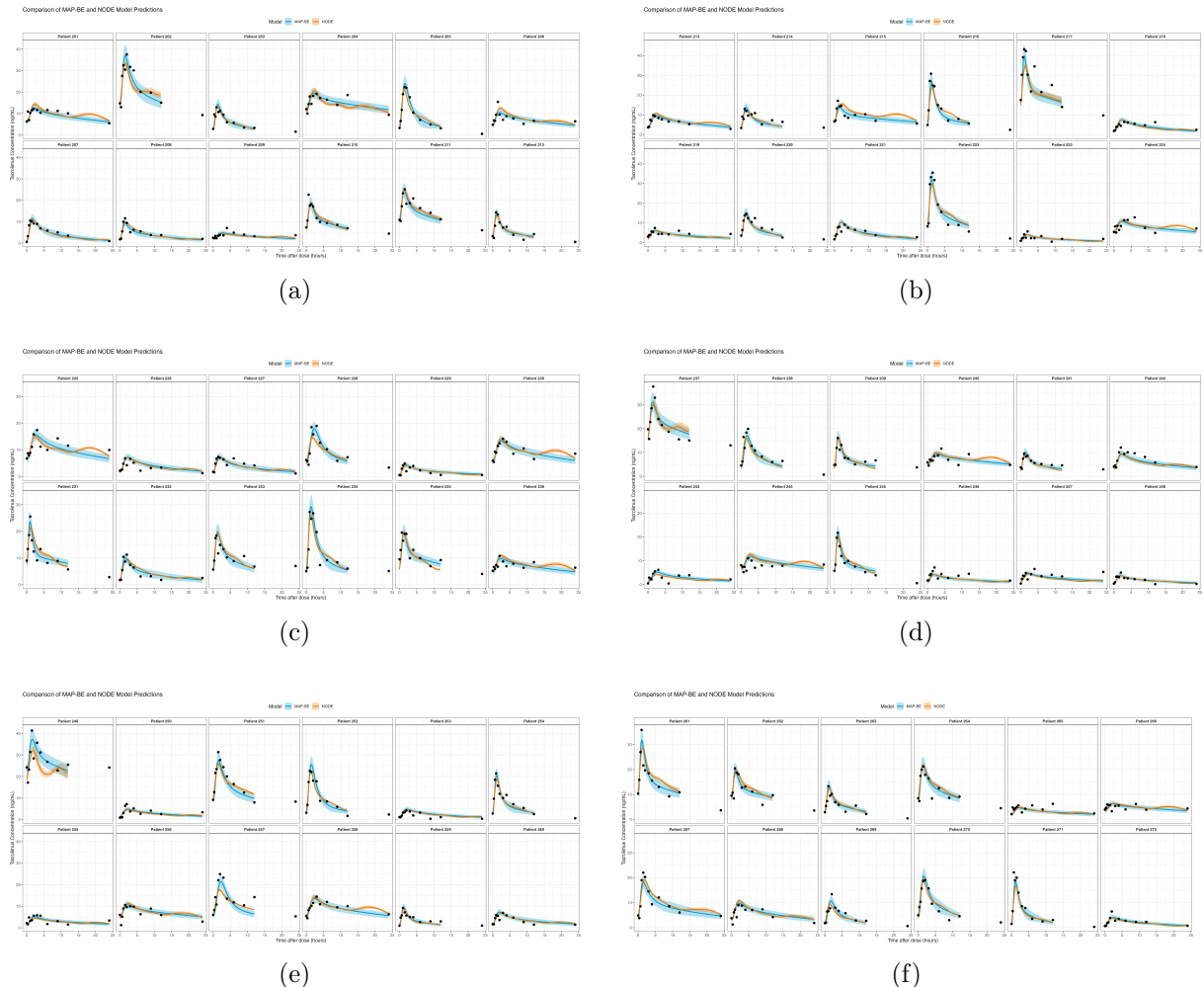


Figure 7: Main caption for all 6 plots. In blue is the prediction of the NMLE+MAP-BE and in orange the one of Neural ODE. Ground truth points are in black.

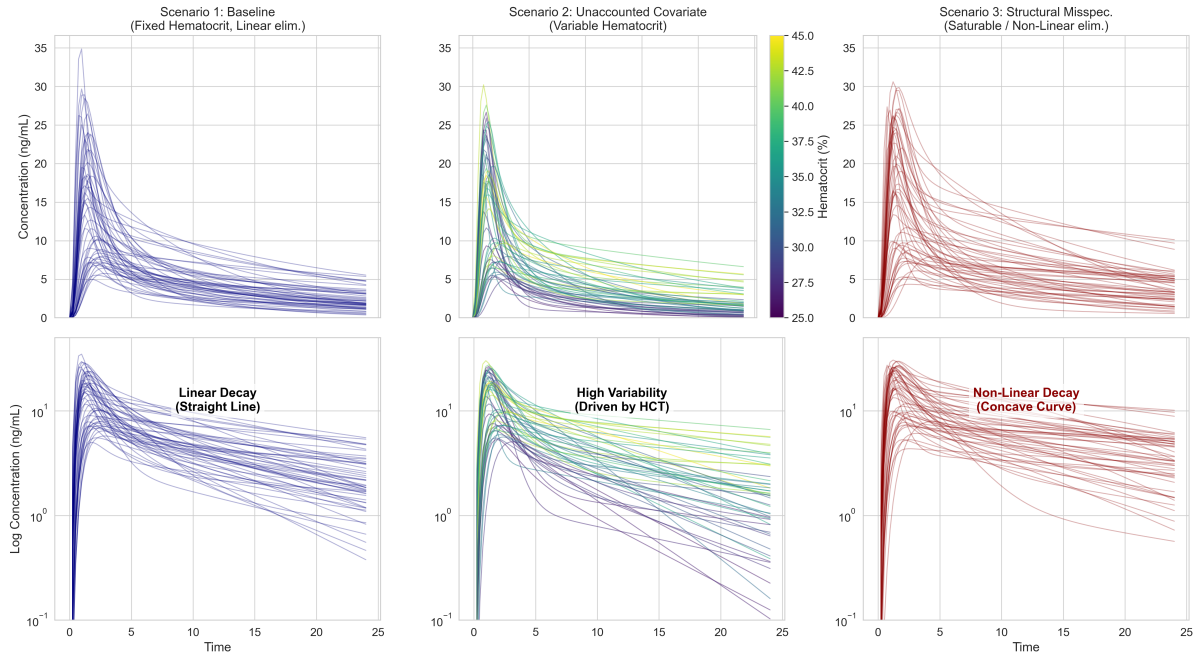


Figure 8: Comparison of ground truth data distributions across the three simulated scenarios. These plots illustrate the underlying concentration data generated for the simulation study. They demonstrate that the distinct physiological mechanisms introduced in Scenario 2 (unaccounted covariate) and Scenario 3 (saturable kinetics) produce plausible patient profiles comparable to the standard baseline (Scenario 1).